Available online at www.sciencedirect.com
SCIENCE DIRECT®
Polymer 45 (2004) 2751–2759
polymer
www.elsevier.com/locate/polymer

Recycled poly(ethylene terephthalate)/layered silicate nanocomposites: morphology and tensile mechanical properties

A. Pegoretti[a,*], J. Kolarik[b], C. Peroni[a], C. Migliaresi[a]

[a]*Department of Materials Engineering and Industrial Technologies, University of Trento, via Mesiano 77, 38050 Trento, Italy*
[b]*Institute of Macromolecular Chemistry, Academy of Sciences of the Czech Republic, 16206 Prague 6, Czech Republic*

Received 26 September 2003; received in revised form 21 January 2004; accepted 11 February 2004

Abstract

Various amounts (1, 3 and 5 wt%) of a non-modified natural montmorillonite clay (Cloisite® Na^+) or of an ion-exchanged clay modified with quaternary ammonium salt (Cloisite® 25A) were dispersed in a recycled poly(ethylene terephthalate) matrix (rPET) by a melt intercalation process. Microphotographs of composite fracture surfaces bring evidence that particles of Cloisite® 25A are much better dispersed in the rPET matrix than those of Cloisite® Na^+. Moreover, WAXS measurements indicate that the lamellar periodicity of Cloisite® 25A is increased in the composites, which evidences intercalation of rPET between silicate layers (lamellae) of the clay. In the case of Cloisite® Na^+, a very small thickening of lamellae due to mixing with rPET indicates only minute intercalation.

Uniaxial tensile tests show that both clays increase the modulus of the rPET composites; more effective Cloisite® 25A accounts for a 30% increase at loading of 5 wt%. Yield strength remains practically unaffected by the used fractions of the clays while tensile strength slightly decreases with the clay content; in parallel, strain at break dramatically drops. Tensile compliance of the composites is virtually independent of applied stress up to 26 MPa. Essential part of the compliance corresponds to the elastic time-independent component, while the viscoelastic component is low corresponding only to a few percent of the compliance even at relatively high stresses. The compliance of the composites is only slightly lower than that of the neat rPET, the reinforcing effect of Cloisite® 25A being somewhat stronger. Both clays have beneficial effect on the dimensional stability of the composites since—in contrast to the neat rPET—the creep rate does not rise at long creep periods.

Keywords: Recycling; Poly(ethylene terephthalate); Nanocomposites

1. Introduction

Key points for most engineering applications of thermoplastics are their thermal stability, stiffness, and strength that can be improved by addition of suitable reinforcing agents such as fibres or fillers. Nevertheless, potential applications of thermoplastic matrices and related composites may be limited by their poor dimensional stability when they are exposed to a long-lasting dead load (constant external force). Thus, the knowledge of their resistance to creep over appropriate intervals of time, stress and temperature is of a great practical interest [1,2]. Many thermoplastics, in particular crystalline ones, show non-linear viscoelastic behaviour even at relatively low strains (smaller than 1%), because the produced strain is no longer linearly proportional to the acting stress (the compliance rises with stress). The stress–strain non-linearity observed in tensile creep experiments can be viewed [3,4] (at least partly) as a consequence of the strain-induced volume dilatation which occurs in materials whose Poisson ratio is smaller than 0.5. Although the creep of many polymeric materials has been described in literature, so far little is known about the creep of polymeric nanocomposites, which represent a new class of polymeric materials. In view of the variability of applications of layered silicate-based nanocomposites, it is highly desirable to have detailed information on their physical properties as functions of composition.

Poly(ethylene terephthalate) (PET) has become one of the major post consumer plastics wastes, in addition to polyethylene, polypropylene, polystyrene, and poly(vinyl

* Corresponding author. Tel.: +36-0461-882452; fax: +39-0461-881977.
E-mail address: alessandro.pegoretti@ing.unitn.it (A. Pegoretti).

0032-3861/$ - see front matter © 2004 Elsevier Ltd. All rights reserved.
doi:10.1016/j.polymer.2004.02.015

chloride) [5]. Large amounts of PET recycled from municipal wastes are currently stimulating its usage in the same demanding applications in which virgin PET has been used. Tensile creep of recycled PET (rPET) blended with impact modifiers was analysed in our previous communication [6]. Although numerous patents have been issued and a number of papers have been published on PET/clay nanocomposites, to date no products have entered the market [7–15]. Moreover, to our knowledge no data have been published on the preparation and characterisation of the rPET/clay nanocomposites.

The objectives of this communication are to study (i) morphology, (ii) uniaxial stress-strain behaviour, and (iii) short-term and long-term creeps of rPET and its nanocomposites with two types of clay (montmorillonite) incorporated in the amounts up to 5 wt%. In particular, we have attempted to evaluate the effects of the clays on produced creep at relatively high stresses that may account for a non-linear stress-strain relation.

2. Format for the creep of polymeric materials

Creep deformation $\varepsilon(t,\sigma,T)$ depending on time t, stress σ and temperature T is usually viewed as consisting of three components [1,2]: (i) elastic (instantaneous) deformation $\varepsilon_e(\sigma,T)$; (ii) viscoelastic (reversible, time-dependent) deformation $\varepsilon_v(t,\sigma,T)$; (iii) plastic (irreversible) deformation $\varepsilon_p(t,\sigma,T)$:

$$\varepsilon(t,\sigma,T)=\varepsilon_e(\sigma,T)+\varepsilon_v(t,\sigma,T)+\varepsilon_p(t,\sigma,T) \tag{1}$$

In practice, the conditions should be avoided where $\varepsilon_p(t,\sigma,T)>0$ because any plastic deformation usually accounts for irreparable damage of an end-product. The corresponding tensile compliance $D(t,\sigma,T)=\varepsilon(t,\sigma,T)/\sigma$ reads:

$$D(t,\sigma,T)=D_e(\sigma,T)+D_v(t,\sigma,T)+D_p(t,\sigma,T) \tag{2}$$

Storage of experimental creep data in a graphical form is impractical. If they can be fitted by an equation, then evaluation of creep rate, interpolation or extrapolation of creep deformation and quantitative description of the effects of external variables are facilitated. Many attempts have been made [16–18] to describe the creep as a product of independent functions of time or stress or temperature, i.e. $D(t,\sigma,T)=C_p g_1(t)g_2(\sigma)g_3(T)$. The parameters of such empirical equations are customarily determined *a posteriori* by fitting experimental data. While $g_1(T)$ is usually identified with the Williams–Landel–Ferry (WLF) or Arrhenius equation, of numerous empirical functions proposed for $g_1(t)$ and $g_2(\sigma)$ we have found [3,4] the following equation [19] suitable for both short- and long-term tensile creeps of PP and its blends:

$$D(t,\sigma)=W(\sigma)(t/\tau_{rm})^n \tag{3}$$

where $W(\sigma)$ is a function of the stress, τ_{rm} is the mean retardation time and $0\le n\le 1$ is the creep curve shape parameter reflecting the distribution of retardation times. We will use Eq. (3) in the following form:

$$\begin{aligned}\log D(t,\sigma)&=[\log W(\sigma)-n\log\tau_{rm}\\&\quad -n\log a_\varepsilon(t)]+n\log(t)\\&=\log C(t,\sigma)+n\log t\end{aligned} \tag{4}$$

The retardation time τ_{rm} is assumed to be controlled by available fractional free volume according to the following equation for the shift factor:

$$\log a=\log[\tau_{rm}(f_2)/\tau_{rm}(f_1)] \tag{5}$$

where $f_2>f_1$ are the fractional free volumes. Obviously, if the free volume changes are small during creep measurements, the shift factor tends to be negligible.

3. Experimental

3.1. Materials

Recycled poly(ethylene terephthalate) (rPET) pellets (density ISO 1183(A); 1.328 g/cm^3; MVR ISO 1133 = 115 ml/10 min; intrinsic viscosity ISO 1628-5 = 0.70 dl/g) were produced by Eco Selekta Italia Srl (Salorno, Italy) from extrusion processing of reclaimed bottles used for beverages.

Two montmorillonite clays (Cloisite® Na$^+$ and Cloisite® 25A) were supplied by Southern Clay Products Inc. (Gonzales, Texas) and used as received. Cloisite® Na$^+$ is a non-modified natural montmorillonite, while Cloisite® 25A is an ion-exchanged clay modified with a quaternary ammonium salt (dimethyl, hydrogenated tallow, 2-ethylhexyl quaternary ammonium) [20].

Composites with 1, 3 and 5% by weight of Cloisite® Na$^+$ or Cloisite® 25A in rPET were prepared by direct melt compounding and moulding in a Sandretto injection moulding machine, model 310/95, (average barrel temperature: 270 °C; injection pressure: 13.5 MPa; mould temperature: 12 °C). ASTM D638 dumb-bell specimens (length: 210 mm; thickness: 3.3 mm; gauge length: 80 mm; gauge width: 12.8 mm) were produced and stored for more than 6 months at room temperature to avoid any interfering effect of the physical ageing during measurements. Specimens for scanning transmission electron microscopy and wide-angle X-ray scattering were cut from the dumb-bell specimens.

3.2. Scanning transmission electron microscopy (STEM)

Dumb-bell specimens were cut in the middle of their length in the direction perpendicular to the injection flow. Afterwards, ultra-thin sections were cut with a microtome (Leica Ultracut UCT) cooled with liquid nitrogen. The

sections were observed in a scanning electron microscope (TS 5130 VEGA, TESCAN) with a transmission adapter.

3.3. Wide-angle X-ray scattering (WAXS)

Wide-angle X-ray scattering was used to evaluate the interaction (intercalation, exfoliation) of the used clays with the rPET matrix. WAXS diffraction patterns were recorded by using the powder diffractometer HZG/4A (Freiberger Preazisionsmechanik, Freiberg, Germany). Reflection measurements of WAXS were carried out with regard to orientation of clay particles in test pieces.

3.4. Uniaxial tensile tests

Uniaxial tensile tests on ASTM-D638 dogbone specimens were conducted by using an Instron 4502 tensile tester equipped with a 10 kN load cell. The initial length of the narrow section of test specimens was about 80 mm; its cross-section was about 12.8 mm × 3.3 mm. Measurements of the modulus were performed at room temperature with an electrical extensometer (Instron, model 2620): a gauge length of 25 mm, cross-head speed of 1 mm/min. Yield and fracture data were evaluated without an extensometer at a cross-head speed of 50 mm/min. All reported properties were evaluated on at least 5 specimens and standard deviation bars (± SD) are reported in the plots.

3.5. Tensile creep measurements

The measurements were performed with dumb-bell specimens (gauge length: 80 mm) by using an apparatus equipped with a mechanical stress amplifier (lever) 11:1. The displacement was measured with a mechanical gauge whose accuracy is about 2 μm, i.e. about 0.0025%. Mechanical conditioning before each creep measurement consisted in applying a stress (for 1 min), which produced a strain larger than the expected final strain attained in the following measurement; the recovery period after the mechanical conditioning was more than 1 h. All creep tests were implemented at room temperature, i.e. 21–23 °C.

Short-term tensile creep measurements in the interval 0.1–100 min were performed with one test specimen at four gradually increasing stress levels (between 5 and 30 MPa) in order to estimate the linearity limit between stress and strain. Each short-term creep measurement was followed by a 22 h recovery before another creep test (at an increased stress) was initiated. Long-term tensile creep experiments under a selected stress extended from 0.1 to 10 000 min. In this case, test specimens were used only for one measurement.

4. Results and discussion

4.1. Morphology

Microphotographs of fracture surfaces of rPET/clay nanocomposites (Fig. 1) show that the prepared materials consist of continuous rPET matrix (light gray areas) and dispersed clay (darker regions). It is quite obvious that the particles of Cloisite® 25A are much finer than those of Cloisite® Na^+. Fig. 1(a) reveals a rather coarse dispersion of Cloisite® Na^+ with particles on a micron scale. On the other hand, Cloisite® 25A clay is much better dispersed in the rPET matrix (Fig. 1(b)); some silicate layers appear to be exfoliated into single layers and randomly dispersed in the polymer matrix.

WAXS measurements (Fig. 2) are in accordance with the STEM microphotographs, indicating that the lamellar periodicity $d_{001} = 1.88$ nm of Cloisite® 25A was increased to $d_{001} = 3.21$ nm in the composite with 5% of Cloisite®

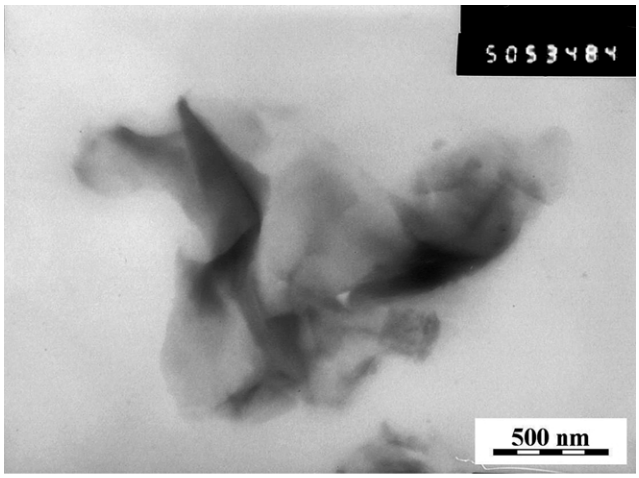

(a)

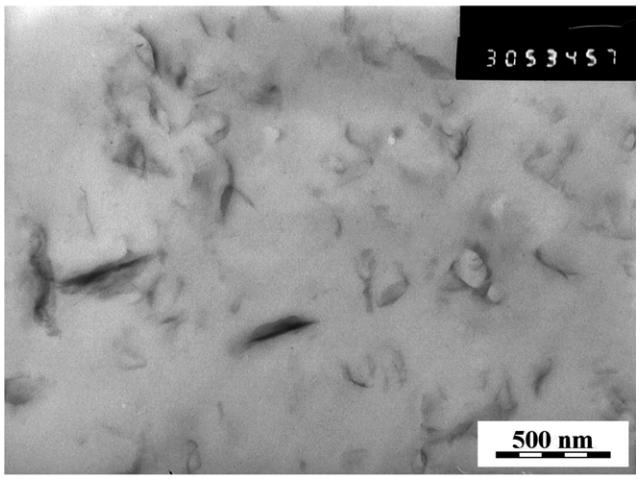

(b)

Fig. 1. STEM microphotographs of the fracture surfaces of rPET composites filled with 5 wt% of: (a) Cloisite® Na^+; (b) Cloisite® 25A.

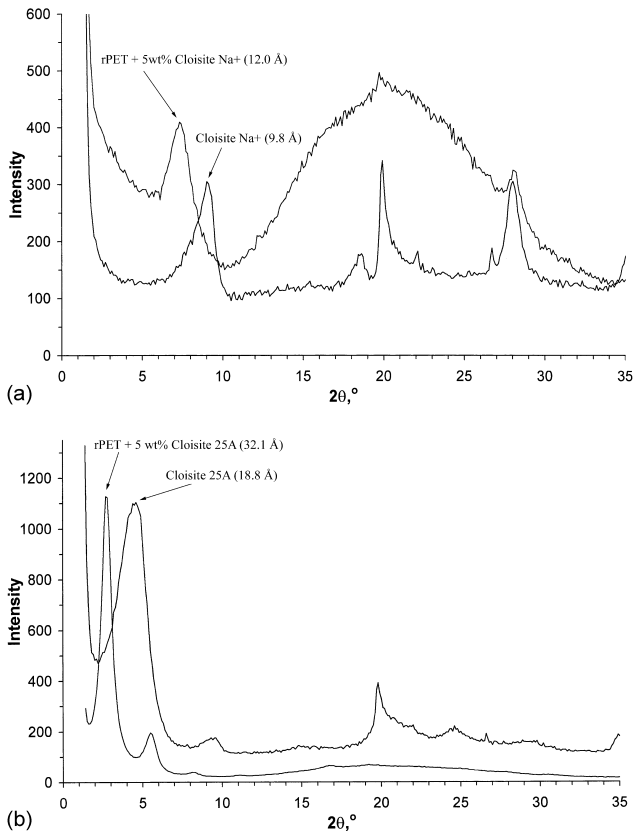

Fig. 2. Wide angle X-ray scattering patters for rPET composites filled with 5 wt% of: (a) Cloisite® Na^+; (b) Cloisite® 25A.

25A, which evidences a strong intercalation of PET between silicate layers (lamellae) of the clay. The intercalated lamellar structure is more ordered than the original one, which is documented by a strong narrowing of the peaks corresponding to the lamellar structure (Fig. 2(b)). In the case of Cloisite® Na^+ with $d_{001} = 0.98$ nm, the intercalation of lamellae due to mixing with PET is much smaller achieving a value of 1.20 nm, which means that the extent of the intercalation is very minute (Fig. 2(a)). It is interesting to note that the lamellar periodicities evaluated by WAXS measurements on both clays before polymer intercalation are in a good accordance with the values reported by the manufacturer ($d_{001} = 1.86$ nm for Cloisite® 25A and $d_{001} = 1.17$ nm for Cloisite® Na^+) [20].

4.2. Stress–strain behaviour

Typical stress–strain curves of rPET nanocomposites loaded with various amounts of Cloisite® 25A clay are reported in Fig. 3. (Stress–strain curves of the rPET/Cloisite® Na^+ nanocomposites are not reported because they are quite analogous.) Unfilled rPET matrix is characterised by extensive deformation after yielding which is obviously related to a low crystallinity of the specimens rapidly cooled during injection in a cold mould. Differential scanning calorimetry indicates a crystalline fraction of about 13 wt% for rPET which is not appreciably

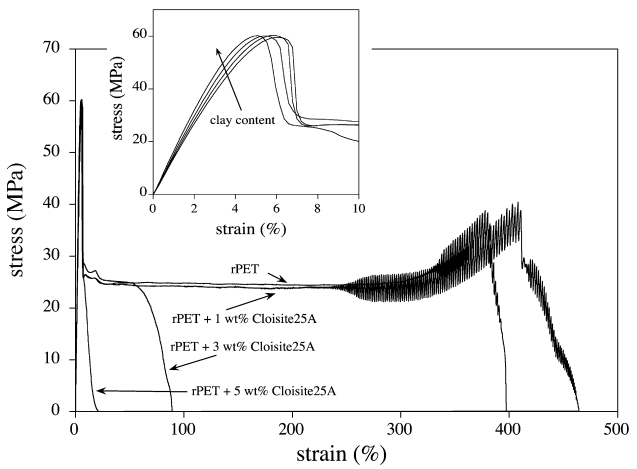

Fig. 3. Typical stress–strain curves of rPET nanocomposites loaded with various amounts of Cloisite® 25A.

affected by clay addition [21]. The fracture of rPET and of the composite with 1 wt % of clay is preceded by a region of load oscillation and cold-drawing. This apparently peculiar behaviour was observed by a number of workers [22]. On amorphous virgin PET film this was shown to be a thermal phenomenon associated with thermal fluctuations in the material neck during cold drawing [22]. Fig. 3 also indicates that the clay addition brings about a small increase in modulus and a reduction of elongation at break.

Fig. 4 shows that Cloisite® 25A is much more efficient in increasing the tensile modulus than Cloisite® Na^+: for a clay content of 5 wt%, the relative modulus (i.e. the ratio of the composite and matrix moduli) is about 1.31 for Cloisite® 25A and about 1.12 for Cloisite® Na^+. It is interesting to note that the addition of 5 wt% of calcium carbonate in the same rPET accounted for a relative modulus of only 1.06 [21]. The higher efficiency of Cloisite® 25A can be explained by better polymer intercalation reached with this ion-exchanged clay in comparison with the non-treated material (as evidenced by STEM and WAXS measurements). It is important to point out that the reinforcing effect of the clays in rPET obtained by melt

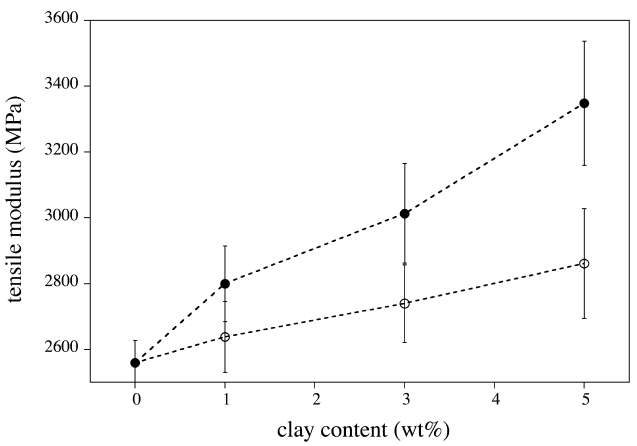

Fig. 4. Tensile modulus as a function of (○) Cloisite® Na^+ and (●) Cloisite® 25A contents.

intercalation directly in the injection molding machine is practically identical with that reported for virgin-PET/clay nanocomposites obtained by melt compounding with co-rotating twin screw extruders and following injection molding [8,13]. On the other hand, an enhanced clay exfoliation and relative modulus of 2.7 for composites with 5 wt% clay were achieved by in situ polymerization of PET monomer on a treated clay [7].

It is instructive to compare our data with the data reported for analogous composites with different matrices. For example, Gopakumar et al. [23] found a relative modulus of about 1.20 for an HDPE matrix grafted with 1 wt% of maleic anhydride and filled with 5 wt% of an ion-exchanged clay (Nanomer® I.44PA). Boucard et al. [24] assessed a relative modulus of 1.36 for polypropylene nanocomposites containing 5 wt% of a organophilic layered silicate (Nanofil 948) and 20 wt% of a maleic anhydride grafted polypropylene as coupling agent. Wang et al. [25] achieved a relative modulus of about 1.52 for polyamide-6 nanocomposites reinforced with 5 wt% of a surface-modified montmorillonite mineral (Nanomer® I.30TC). Liu et al. [26] ascertained a relative modulus of about 1.37 for polyamide-6 nanocomposites loaded with 4.2 wt% of an organically modified montmorillonite mineral. In the case of polyamide-6, relative modulus values of 1.52–1.81 [27] and 2.12 [28] have recently been found for nanocomposites obtained by melt-intercalation of about 5 wt% of organically modified montmorillonites. In some cases, even if a partial intercalation and exfoliation was obtained the stiffening effect was less pronounced, as documented by Wan et al. [29] who determined a relative modulus of only 1.05 for PVC nanocomposites filled with 5 wt% of an organically-modified montmorillonite. As can be seen, the relative modulus of melts compounded thermoplastic nanocomposites based on montmorillonite clays strongly depends on the matrix type and processing conditions.

The yield strength of rPET nanocomposites is not affected by the incorporated fraction of both types of the clay (Fig. 5), which evidences a good interfacial adhesion. Besides, it can be observed that the clays slightly reduce the tensile strength of the composites; a higher value found for the composite with 5 wt % of the clays is solely due to the fact that these materials fail immediately after yielding (Fig. 3). The detrimental effect of the clay fraction on the rPET ultimate mechanical properties is also evidenced by the reduction of the strain at yield and strain at break (Fig. 6). A profound reduction of the strain at break was also observed for other polymer/clay nanocomposites obtained by melt-intercalation process [27,28,30–32]. Thus, we can see that the plastic deformation of polymer matrices is generally suppressed by an increase in the clay fraction.

4.3. Short-term tensile creep

Creep behaviour of polymer nanocomposites is of paramount importance from the viewpoint of their dimensional stability. To measure the creep of polymeric materials in the region of linear viscoelasticity, it is inevitable to perform creep experiments at very low strain levels in order to obtain log D(t) vs. log t plots independent of applied stress. However, such approach is impractical because (i) the linearity limit between stress and strain is usually very low (a few tenths of %) and uncertain, (ii) relative accuracy of the creep measurements in this region is low and (iii) the effect of stress remains unspecified, which is a serious shortcoming from the practical point of view. Therefore, we performed our experiments at relatively high stresses that can be encountered in applications of various end products.

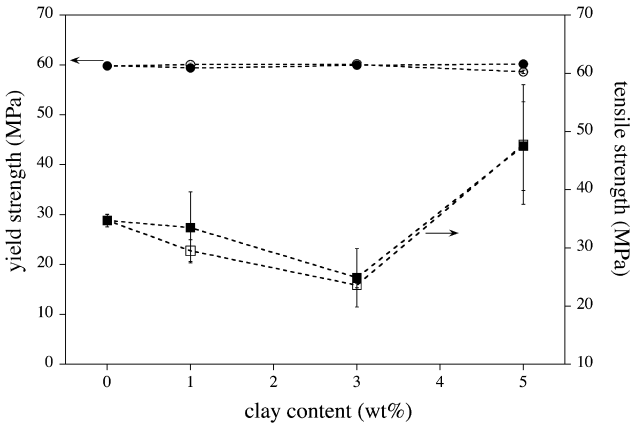

Fig. 5. Yield strength (circles) and tensile strength (squares) as functions of clay content. Open and full points refer to Cloisite® Na^+ and Cloisite® 25A, respectively.

Tensile compliance $D(t)$ of unfilled rPET (Fig. 7, Table 1) is virtually independent of applied stress (up to 26 MPa), which indicates linear viscoelastic behavior. Essential part of the strain produced by applied loads corresponds to the elastic time-independent component, which occurs immediately after loading. Viscoelastic compliance $D_v(t)$ is low representing only a few percent of the compliance $D(t)$. For this reason, the measurements of $D_v(t)$—particularly at low stresses—are rather inaccurate, which may result in

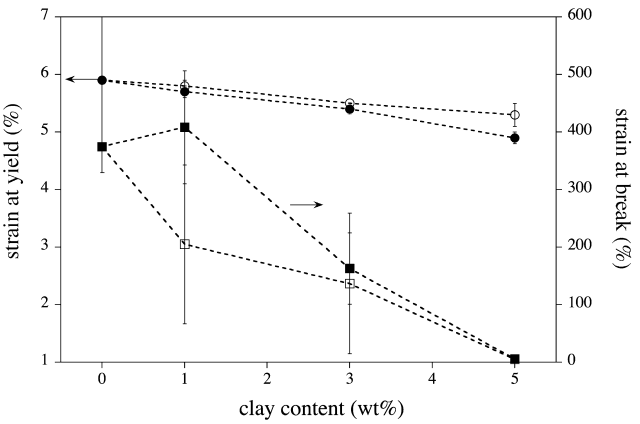

Fig. 6. Strain at yield (circles) and strain at break (squares) as functions of clay content. Open and full points refer to Cloisite® Na^+ and Cloisite® 25A, respectively.

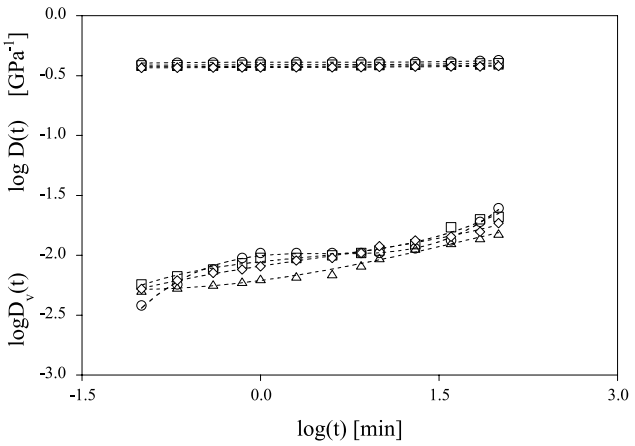

Fig. 7. Short-term creep of unfilled rPET (sample 1 in Table 1): effect of stress on compliance $D(t)$ (upper part) and its viscoelastic component $D_v(t)$ (lower part). Applied tensile stress (MPa): (○) 6.22; (□) 12.45; (△) 18.67; (◇) 24.89.

apparently irregular effects of stress on the log $D_v(t)$ vs. log t dependencies.

The effect of four selected stress levels on the time dependencies of $D(t)$ in two series of the rPET nanocomposites loaded with Cloisite® Na^+ and Cloisite® 25A is summarized in Table 1. As an example, the compliance time dependencies for the composites with 5 wt% of Cloisite® Na^+ and Cloisite® 25A are reported in Figs. 8 and 9, respectively. Studied composites have somewhat lower compliance than rPET; the effect of applied stress on $D(t)$ is very small, which accounts for irregularities in the values of log C in Table 1. Nonetheless it can be said that the composites display quasi-linear viscoelastic behavior, which also means that the effect of strain-induced free volume in Eq. (4) is negligible.

If the values of log C for the highest applied stress are compared (they are relatively more accurate than the values obtained at lower stresses and/or strains), it comes out that the effect of Cloisite® Na^+ is practically negligible, while the compliance slightly decreases with the content of Cloisite® 25A. These results are in conformity with the morphology analysis and uniaxial tensile tests previously discussed. Only the rise of $D_v(t)$ with applied stress might be viewed as an indication of the non-linear viscoelastic behavior of PET nanocomposites in the interval of applied stresses. Table 1 also evidences that the prepared composites show very low values of the parameter n, i.e. of the

Table 1
Effect of tensile stress on the parameters characterizing the compliance of composites poly(ethylene terephthalate)/clay

Sample	Type of clay	Clay content (wt%)	Stress (MPa)	log C	n	R^2
1	None	0	6.22	−0.3888	0.0051	0.7559
			12.45	−0.4093	0.0051	0.8599
			18.67	−0.4224	0.0039	0.8991
			24.89	−0.4317	0.0046	0.9490
2	Cloisite® Na^+	1	6.54	−0.3913	0.0050	0.9722
			13.08	−0.4145	0.0062	0.9029
			19.62	−0.4288	0.0042	0.9506
			26.16	−0.4260	0.0047	0.9303
3	Cloisite® Na^+	3	5.90	−0.5053	0.0085	0.8822
			11.79	−0.4718	0.0074	0.8706
			17.69	−0.4605	0.0056	0.9711
			23.58	−0.4392	0.0080	0.9001
4	Cloisite® Na^+	5	6.35	−0.5393	0.0063	0.9291
			12.69	−0.4843	0.0041	0.8146
			19.04	−0.4720	0.0073	0.9356
			25.38	−0.4346	0.0081	0.9586
5	Cloisite® 25A	1	5.97	−0.5696	0.0092	0.7755
			11.94	−0.4742	0.0056	0.9400
			17.91	−0.4491	0.0061	0.9353
			23.88	−0.4301	0.0069	0.9367
6	Cloisite® 25A	3	6.49	−0.5616	0.0119	0.9840
			12.97	−0.5104	0.0071	0.9252
			19.46	−0.4938	0.0055	0.9338
			25.95	−0.4725	0.0077	0.9526
7	Cloisite® 25A	5	6.28	−0.5836	0.0100	0.9639
			12.56	−0.5410	0.0070	0.9627
			18.84	−0.5249	0.0066	0.9709
			25.12	−0.4985	0.0088	0.9599

C, n, parameters of Eq. (4). R : reliability values.

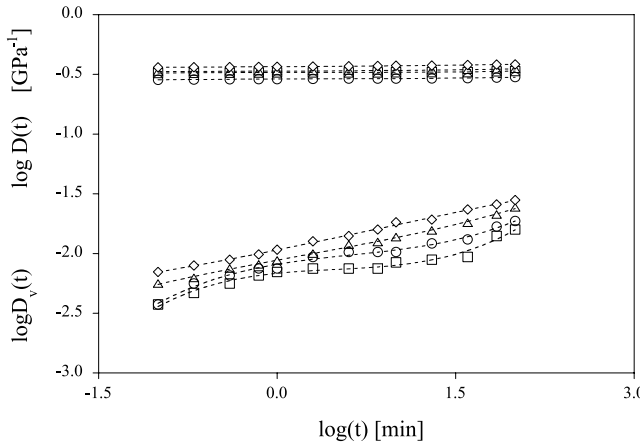

Fig. 8. Short-term creep of PET with 5% Cloisite® Na^+ (sample 4 in Table 1): effect of stress on compliance $D(t)$ (upper part) and its viscoelastic component $D_v(t)$ (lower part). Applied tensile stress (MPa): (○) 6.35; (□) 12.69; (△) 19.04; (◇) 25.38.

slope of the log $D(t)$ vs. log t plots, which are comparable with that of rPET. Thus, it is difficult to see any clear-cut dependence of the parameter n on (i) the applied stress or (ii) the content of clay in composites. For these reasons it was necessary to carry out the long-term creep experiments.

4.4. Long-term tensile creep

Table 2 and Figs. 10 and 11 make it clear that the effects of clay concentration on the tensile creep are rather limited. As we can see, Eq. (4) fits well log $D(t)$ plotted against log t thus evidencing a negligible role of the strain-induced free volume also in the long-term creep experiments. The effect of Cloisite® Na^+ on $D(t)$ is negligible because all plots in Fig. 11 overlap, while log C in Table 2 exhibits a subtle decrease with clay content. Larger decrease in log C with the clay fraction can be seen in Table 2 for the composites with Cloisite® 25A. However, mild stiffening effects of the clays seem to be compensated by rising parameter n. Thus

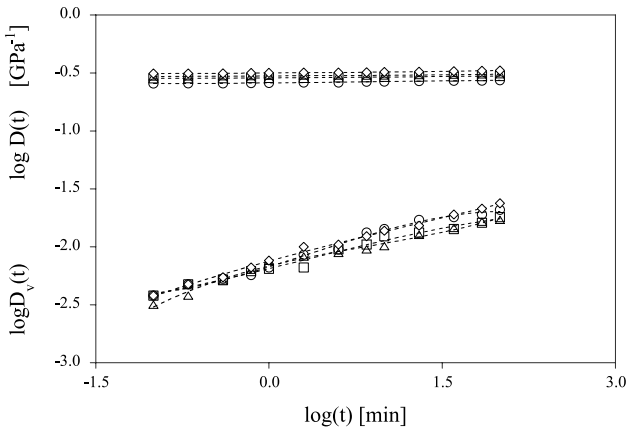

Fig. 9. Short-term creep of PET with 5% Cloisite® 25A (sample 7 in Table 1): effect of stress on compliance $D(t)$ (upper part) and its viscoelastic component $D_v(t)$ (lower part). Applied tensile stress (MPa): (○) 6.28; (□) 12.56; (△) 18.84; (◇) 25.12.

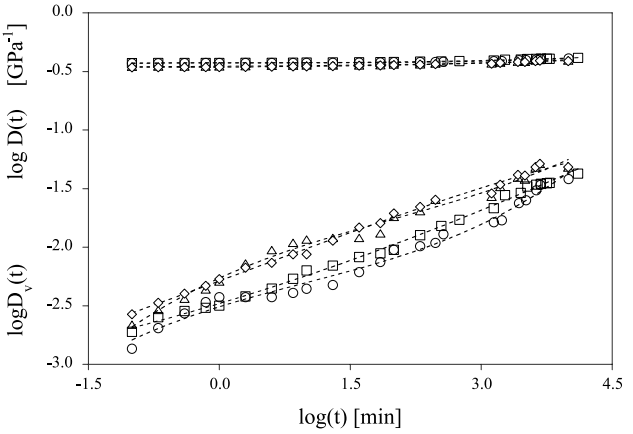

Fig. 10. Long-term creep of rPET composites: effect of clay fraction on compliance $D(t)$ (upper part) and its viscoelastic component $D_v(t)$ (lower part). Weight fraction of Cloisite® Na^+ and applied tensile stress (MPa): (○) 0 wt%, 17.42; (□) 1 wt%, 18.31; (△) 3 wt%, 16.51; (◇) 5 wt%, 17.77.

we can conclude that the reinforcing effect of both types of the clay is rather small in the range of tested compositions. On the other hand, no noticeable upswing of log $D(t)$ with log t for longer creep periods ($t > 1000$ min) can be seen in Figs. 10 and 11, which was typical of the blends rPET/impact modifier described in our previous communication [6]. Also the recovery following the long-term creep experiments has proved complete reversibility of the produced deformations. Thus, a positive effect of clays in the rPET matrix can be seen in that the creep rate does not rise at long creep periods.

5. Conclusions

Microphotographs of fracture surfaces of the rPET/clay nanocomposites show that the particles of Cloisite® 25A (ion-exchanged montmorillonite) are much better dispersed in the matrix than particles of Cloisite® Na^+ (natural

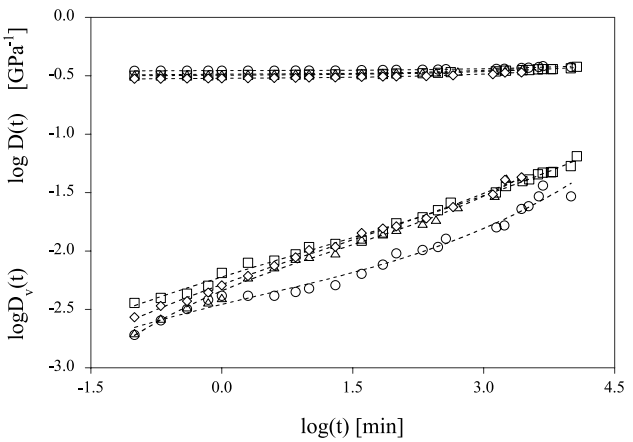

Fig. 11. Long-term creep of rPET composites: effect of clay fraction on compliance $D(t)$ (upper part) and its viscoelastic component $D_v(t)$ (lower part). Weight fraction of Cloisite® 25A and applied tensile stress (MPa): (○) 0 wt%, 17.42; (□) 1 wt%, 18.10; (△) 3 wt%, 18.16; (◇) 5 wt%, 17.59.

Table 2
Effect of the composition on the parameters characterizing the long-term compliance of composites poly(ethylene terephthalate)/clay

Sample	Type of clay	Clay content (wt%)	Stress (MPa)	log C	n	R^2
1	None	0	17.42	−0.4293	0.0070	0.7782
2	Cloisite® Na^+	1	18.31	−0.4283	0.0086	0.8618
3	Cloisite® Na^+	3	16.51	−0.4570	0.0112	0.8896
4	Cloisite® Na^+	5	17.77	−0.4631	0.0118	0.9047
5	Cloisite® 25A	1	16.71	−0.4981	0.0135	0.8830
6	Cloisite® 25A	3	18.16	−0.4904	0.0141	0.8566
7	Cloisite® 25A	5	17.59	−0.5242	0.0148	0.8996

C, n : parameters of Eq. (4). R : reliability values.

montmorillonite). In parallel, the WAXS measurements indicate a markedly increased lamellar periodicity of Cloisite® 25A in the composites, which evidences intercalation of rPET between silicate layers (lamellae) of the clay. In the case of Cloisite® Na^+, a very small thickening of lamellae due to mixing with rPET evidences only a minute intercalation.

Mechanical properties of the prepared composites are in a good correlation with observed morphologies. Although both clays cause a modulus increase of the rPET composites, this effect is stronger for the organically treated clay. It is essential that the yield strength is not reduced the clay addition, which is a sign of a good interfacial adhesion. Stress at break slightly decreases while strain at break dramatically drops with the clay fraction. Creep compliance of PET and prepared composites is virtually independent of the applied tensile stress up to 26 MPa, which indicates a good dimensional stability. Essential part of the strain of these materials produced by an applied load corresponds to the elastic time-independent component, which occurs immediately after loading; the viscoelastic component of the compliance is low corresponding only to a few percent of the compliance. The composites exhibit a slightly lower compliance than rPET; a stronger reinforcing effect of Cloisite® 25A in comparison with that of Cloisite® Na^+ is manifested by a lower compliance. Long-term creep measurements prove a beneficial effect of the clays on the dimensional stability because the creep rate of the composites does not increase at long creep periods ($t > 1000$ min), which was typical of PET blends with impact modifiers.

Acknowledgements

This work was carried out with the financial support of the 'Ministero dell'Istruzione dell'Università e della Ricerca' (MIUR - Italy), COFIN 2000 (Grant No. MM09012922_005). The second author (J.K.) is indebted to the Grant Agency of the Academy of Sciences of the Czech Republic for financial support of this work (Grant No. A4050105). The authors sincerely wish to thank Mr Gerardo Lopez of Southern Clay Products Inc. for supplying montmorillonite minerals for this study and Dr Miroslav Slouf and Dr Josef Baldrian from the Institute of Macromolecular Chemistry, Academy of Sciences of the Czech Republic, for the STEM and WAXS measurements, respectively.

References

[1] Nielsen LE, Landel RF. Mechanical properties of polymers and composites, 2nd ed. New York: Marcel Dekker; 1994.
[2] Crawford RJ. Plastics engineering. Oxford, Oxford: Butterworth-Heinemann; 1998.
[3] Kolarík J, Pegoretti A, Fambri L, Penati A. J Appl Polym Sci 2003; 88(3):641–51.
[4] Kolarík J. J Polym Sci, B: Polym Phys 2003;41(7):736–48.
[5] Lin CC. Macromol Symp 1998;135:129–35.
[6] Pegoretti A, Kolarík J, Gottardi G, Penati A. Polym Int 2004.
[7] Ke Y, Long C, Qi Z. J Appl Polym Sci 1999;71:1139–46.
[8] Tsai T-Y. Polyethylene terephthalate–clay nanocomposites. In: Pinnavaia TJ, Beall GW, editors. Polymer–clay nanocomposites. Chichester UK: Wiley; 2000. p. 173–206.
[9] Matayabas JC, Turner SR. Nanocomposite technology for enhancing the gas barrier of polyethylene terephthalate. In: Pinnavaia TJ, Beall GW, editors. Polymer–clay nanocomposites. Chichester UK: Wiley; 2000. p. 207–26.
[10] Ou CF, Ho MT, Lin JR. J Polym Res 2003;10:127–32.
[11] Imai Y, Inukai Y, Tateyama H. Polym J 2003;35(3):230–5.
[12] Zhang GZ, Shichi T, Takagi K. Mater Lett 2003;57:1858–62.
[13] Sanchez-Solis A, Garcia-Rejon A, Manero O. Macromol Symp 2003; 192:281–92.
[14] Davis CH, Mathias LJ, Gilman JW, Schiraldi DA, Shields JR, Trulove P, Sutto TE, Delong HC. J Polym Sci, B: Polym Phys 2002;40: 2661–6.
[15] Boesel LF, Pessan LA. Mater Sci Forum 2002;403:89–93.
[16] Schlimmer M. Rheol Acta 1979;18:62–74.
[17] Boey FYC, Lee TH, Khor KA. Polym Test 1995;14:425–38.
[18] Li JX, Cheung WL. J Appl Polym Sci 1995;56:881–8.
[19] Garbella RW, Wachter J, Wendorff JH. Prog Colloid Polym Sci 1985; 71:164–72.
[20] http://www.nanoclay.com/data/25A.htm; http://www.nanoclay.com/data/Na.htm.
[21] Pegoretti A. Unpublished results.
[22] Boyce MC, Haward RN. The post-yield deformation of glassy polymers. In: Haward RN, Young RJ, editors. The physics of glassy polymers, 2nd ed. London: Chapman and Hall; 1997. Chapter 5.
[23] Gopakumar TG, Lee JA, Kontopoulou M, Parent JS. Polymer 2002; 43:5483–91.
[24] Boucard S, Duchet J, Gerard JF, Prele P, Gonzaalez S. Macromol Symp 2003;194:241–6.

[25] Wang H, Zeng CC, Elkovitch M, Lee LJ, Koelling KW. Polym Eng & Sci 2001;41(11):2036–46.
[26] Liu LM, Qi ZN, Zhu XG. J Appl Polym Sci 1999;71:1133–8.
[27] Uribe-Arocha P, Mehler C, Puskas JE, Altstädt V. Polymer 2003;44: 2441–6.
[28] Liu XH, Wu QJ, Berglund LA, Lindberg H, Fan JQ, Qi ZN. J Appl Polym Sci 2003;88:953–8.
[29] Wan CY, Qiao XY, Zhang Y, Zhang YX. Polym Test 2003;22: 453–61.
[30] Chen L, Wong S-C, Pisharath S. J Appl Polym Sci 2003;88:3298–305.
[31] Wang KH, Koo CM, Chung IJ. J Appl Polym Sci 2003;89:2131–6.
[32] Wang KH, Choi MH, Koo CM, Xu MZ, Chung IJ, Jang MC, Choi SW, Song HH. J Polym Sci, B: Polym Phys 2002;40:1454–63.